ChemComm

RSC Publishing

COMMUNICATION

View Article Online
View Journal | View Issue

Interfacial strain-promoted alkyne–azide cycloaddition (I-SPAAC) for the synthesis of nanomaterial hybrids†

Cite this: *Chem. Commun.*, 2013, **49**, 3982

Received 4th March 2013,
Accepted 22nd March 2013

DOI: 10.1039/c3cc41634h

www.rsc.org/chemcomm

Pierangelo Gobbo,[a] Samantha Novoa,[a] Mark C. Biesinger[b] and Mark S. Workentin*[a]

An *interfacial* strain promoted azide–alkyne cycloaddition (I-SPACC) is introduced as a method to prepare robust nanomaterial hybrids. This is demonstrated with a reaction between a novel dibenzocyclooctyne-modified single walled carbon nanotubes (DBCO-SWCNT) and a versatile water-soluble azide modified gold nanoparticle (N_3-EG_4-AuNP).

Bioorthogonal reactions are a subclass of click reactions that address the strict requirements of biocompatibility. They represent a powerful tool in chemical biology for *in vivo* imaging and tracking of biomolecules, providing unique insights into spatial and temporal aspects of biological processes that cannot otherwise be achieved through traditional biochemical methodologies.[1–3] The most famous bioorthogonal reaction is the copper-free [3+2] Huisgen cycloaddition, also know as strain-promoted alkyne–azide cycloaddition (SPAAC), introduced by C. R. Bertozzi.[4] This reaction was designed to take place rapidly and selectively inside biosystems, solving the problems related to the use of copper in the Cu-catalyzed version of this reaction.[5–7] Thanks to the extremely fast kinetics, the high efficiency, and the biocompatibility coupled with the orthogonality conferred by the ring strain of the cyclooctyne moiety that is the centrepiece of this approach,[8] the SPAAC reaction has been exploited to label *in vivo* azide-modified proteins directly expressed in the cell's cytosol or metabolically functionalized on the cell's membrane.[9–13] The characteristics that make this bioorthogonal reaction desirable in the bioorganic chemistry field, are transferrable to materials chemistry. Indeed, such a fast, clean and orthogonal reaction has the potential to become an important tool for the synthesis of nanostructured systems that require expensive starting materials like nanoparticles and other nanomaterials to react efficiently together without the need for metal catalysts. Despite the great potential of this reaction in the material chemistry field, it has not been used interfacially to prepare hybrid nanomaterials. Indeed only a few applications in materials science have been described. Turro and co-workers used the SPAAC reaction to synthesize photodegradable star polymers,[14] Bernardin *et al.* synthesized monosaccharide-functionalized quantum dots for *in vivo* metabolic imaging through the reaction between cyclooctyne-modified quantum dots and azide-modified monosaccarides,[15] and Popik prepared dibenzocyclooctyne (DBCO)-modified glass, silicon and quartz surfaces, and showed their potential as platforms for the generation of multicomponent surfaces.[7,16]

Here we introduce the concept of an *interfacial* strain-promoted alkyne–azide cycloaddition (I-SPAAC) reaction in carbon based material chemistry, showing for the first time that it can successfully take place at the interface between different nanomaterials. To show this innovative application of the SPAAC reaction, as a proof of concept we prepared a gold nanoparticle (AuNP)–carbon nanotube (CNT) hybrid, which represent a desirable nanomaterial that is gaining always more importance in material chemistry because of its numerous applications in catalysis, sensing and nanomedicine, and its preparation still represents a challenge for material chemists.[17–20] In order to prepare the AuNP–CNT hybrid through the I-SPAAC reaction we synthesized two novel and versatile partner nanomaterials, namely a small (3 nm) *water-soluble* azide-modified AuNP (N_3-EG_4-AuNP) and a DBCO-modified single walled CNT (DBCO-SWCNT), that could give the final product by simply reacting at room temperature and in water media, where both form stable solutions. The final nanohybrid synthesized through the I-SPAAC reaction was easy to prepare, robust, and homogeneously covered with small AuNP as shown by transmission electron microscopy (TEM) and X-ray photoelectron spectroscopy (XPS).

The preparation of N_3-EG_4-AuNP, required first preparing the starting water-soluble gold nanoparticles (Me-EG_3-AuNP) using a modified Brust–Schiffrin method following the previously reported procedure.[21] The azide ligands N_3-EG_4-SH, whose

[a] *Department of Chemistry and Centre for Advanced Materials and Biomaterials, The University of Western Ontario, 1151 Richmond St., London, ON, Canada N6A 5B7. E-mail: mworkent@uwo.ca; Tel: +1-519-661-2111 Ext. 86319*
[b] *Surface Science Western, The University of Western Ontario, 999 Collip Circle, London, ON, Canada N6G 0J3*

† Electronic supplementary information (ESI) available: Synthetic and characterization details, especially for N_3-EG_4-AuNP, ^{1}H and ^{13}C spectra, TEM of N_3-EG_4-AuNP and XPS and high resolution XPS data and FTIR analysis of hybrids. See DOI: 10.1039/c3cc41634h

synthetic details are reported in the ESI,† were introduced onto the Me-EG_3-AuNP using a place-exchange reaction. In a typical synthesis 42.5 μmol of N_3-EG_4-SH were stirred for 20 min in acetone and in presence of the 50.0 mg of basic Me-EG_3-AuNP. The free thiols were subsequently removed by repeatedly washing the dried AuNP film with hexanes and isopropanol. These novel N_3-EG_4-AuNP exhibited the solubility properties of the Me-EG_3-AuNP, forming stable solutions and being readily re-dissolvable in H_2O, acetone, acetonitrile, methanol, ethanol, DMF, DMSO and DCM with no to little aggregation. The N_3-EG_4-AuNPs were characterized using ^{1}H NMR and IR spectroscopy, TGA, and TEM. The ^{1}H NMR spectrum recorded in D_2O exhibited the broad peaks typical of organic modified AuNP, and after place-exchange reaction it showed the appearance of a new resonance at 3.45 ppm related to the methylene protons alpha to the incorporated azide (Fig. S4, ESI†). The ^{1}H NMR spectrum was also recorded in d_3-acetonitrile showing the same characteristics but having better resolved peaks (Fig. S5, ESI†). Through the integration of the peak related to the protons alpha to the azide (3.39 ppm in d_3-acetonitrile) and that of the peak related to the methyl unit of Me-EG_3-SH ligands (3.31 ppm in d_3-acetonitrile) it was possible to estimate the incorporation of 35% azide ligands on the AuNP surface. The IR spectrum of the purified N_3-EG_4-AuNP compared to that of the starting Me-EG_3-AuNP (Fig. S8, ESI†), showed the appearance of the expected asymmetrical stretching of the azide group at 2101 cm^{-1}, confirming the successful functionalization of the basic AuNP. From the analysis of the TGA data (Fig. S9, ESI†), and in particular from the increased percentage of the organic component related to the addition of [CHN_3] units (corresponding to 55.03 g mol^{-1}) through the place-exchange reaction, it was possible to calculate that the AuNP organic shell is composed of 65% of Me-EG_3-S^- ligands, and 35% of N_3-EG_4-S^- ligands, supporting the analysis of the ^{1}H NMR spectroscopy. From the TGA data and from the molecular weight of the two ligands, it was possible to calculate that per milligram of N_3-EG_4-AuNP there are 0.745 μmol of azide ligands. TEM images (Fig. S6, ESI†) showed that the average diameter of the N_3-EG_4-AuNP was 3.22 ± 0.50 nm. From the combination of ^{1}H NMR spectroscopy, TEM and the TGA data, and assuming that the nanoparticles have a spherical shape and that their size is mono-dispersed, it is possible to calculate a nanoparticle raw formula[21] of Au_{1000} (Me-EG_3-S)$_{455}$ (N_3-EG_4-S)$_{245}$.

The novel SWCNT-DBCO were synthesized through a coupling reaction between the carboxylic groups already present on the nanotube's sidewalls and the commercially available DBCO-amine (for details see ESI†). It is noteworthy that it is not necessary to pre-treat or oxidize the CNT before the coupling reaction. The amount of carboxylic groups already present on the CNT sidewalls allows for an efficient functionalization of the carbonaceous material (*vide infra*). The DBCO-modified CNT was found to form stable dispersions in both water and polar organic solvents like DCM, ACN, acetone and ethanol. The SWCNT-DBCO was characterized by XPS and IR spectroscopy. The XPS spectrum of SWCNT-DBCO (Fig. S10b, ESI†) compared to that of the starting material (Fig. S10a, ESI†) clearly shows the appearance of the peak related to the amide

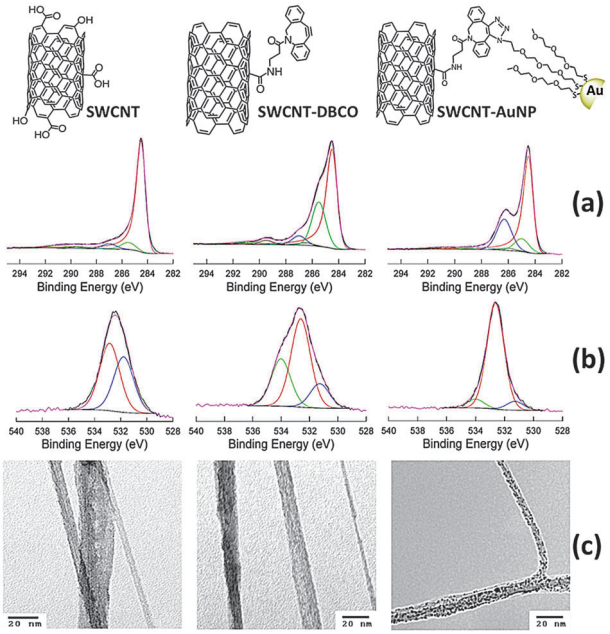

Fig. 1 Top: schematic representation of the nanomaterials used/prepared; (a): high resolution C 1s XPS spectra, (b) high resolution O 1s XPS spectra and (c) TEM images (scale 20 nm) for SWCNT (left), SWCNT-DBCO (centre), SWCNT-AuNP hybrid (right), respectively.

nitrogen at 400.0 eV (1s). The high resolution scan of the carbon 1s (Fig. 1a) and oxygen 1s peaks (Fig. 1b) for the SWCNT-DBCO (centre) compared to that of the SWCNT starting material (left) confirms the successful synthesis of DBCO-modified CNT. The high-resolution scan of the carbon peak shows the appearance of a shoulder at 285.51 eV related to the sp_3-hybridized carbons introduced with the coupling reaction. This is also confirmed by the appearance of a shoulder at 534.01 eV on the high resolution scan of the oxygen peak related to the –(C═O*)–NH–, and by a marked decrease of the –(C═O*)–OH peak (531.28 eV), with respect to the steady component at 532.61 eV of the –C–OH. The IR spectrum of the purified SWCNT-DBCO further confirms this result showing the peaks related to the C–H stretching of the sp_3-hybridized carbons of the DBCO-amine at 2949, 2919, and 2848 cm^{-1}, and a band at 1580 cm^{-1} related to the stretching mode of the amide C═O.

The title SWCNT–AuNP hybrid nanomaterial was then easily prepared through the bioorthogonal I-SPAAC reaction between the two partners: SWCNT-DBCO and the N_3-EG_4-AuNP. The interfacial cycloaddition reaction was carried out simply by mixing the SWCNT-DBCO with the N_3-EG_4-AuNP in water media. In a typical synthesis, to a 1 ml of the SWCNT-DBCO mother solution was added 4 mg of N_3-EG_4-AuNP and the reaction volume was diluted to 4 ml with PBS pH 7 buffer. The system was stirred for 1 hour at room temperature and then the SWCNT–AuNPs were centrifuged in a Pyrex centrifuge test tube. The supernatant was removed, and the decorated CNT were dispersed in water, sonicated for 10 minutes and centrifuged. Subsequently, water was substituted first with acetone, then with dichloromethane (DCM), and the washing procedure (sonication in DCM and centrifugation) was repeated

four more times. This protocol was to ensure removal of any non-covalently bound AuNP. The successful synthesis and purification of the covalent SWCNT–AuNP hybrid was confirmed by XPS and TEM. The XPS spectrum of SWCNT–AuNP (Fig. S10c, ESI†) shows the appearance of the peaks from Au at 84 eV (4f), 334–353 eV (4d), 547–643 eV (4p), and 762 eV (4s), and from S at 162.9 eV (2p) and 228 eV (2s). The high-resolution carbon 1s spectrum (Fig. 1a, right) shows a marked increase of the component at 286.30 eV related to the C–O–C of the AuNP glycol units, while the high-resolution oxygen 1s spectrum (Fig. 1b, right) shows an increase of the corresponding component at 532.63 eV. The Au 4f7/2 core line of AuNP is at 84.5 eV, this binding energy is shifted upwards from that of bulk Au (83.95 eV) due to particle size effects (Fig. S13, ESI†).[22,23] The N 1s core line after the interfacial I-SPAAC reaction shows a new component centered at 401.08 eV (Fig. S13, ESI†). While the major component at 399.98 eV is due to the DBCO-CNT amide nitrogens and to the nitrogen of the triazole rings; this new component is most likely related to the formation of $-NH_3^+$ as a consequence of the photolysis of the unreacted $-N_3$ by the high energy incident radiation.[24] TEM images of the hybrid nanomaterial (Fig. 1c, right) show that AuNP are dispersed on the CNT surface, that they kept their original size and shape, and that there are no unbound particles present, confirming the efficiency of our purification procedure. Indeed, the use of sonication favours the detachment of the AuNP that are only physisorbed on the CNT leaving just those that are covalently bonded.

To further exclude the possibility of unspecific physisorption or bonding of the AuNP to the SWCNT-DBCO, a control experiment was carried out under identical conditions and following the same experimental procedure but using the model Me-EG_3-AuNP instead of the N_3-EG_4-AuNP. The Me-EG_3-AuNP, with the absence of the azide functionalities, is not expected to react with the DBCO-modified CNT because they cannot undergo the I-SPAAC reaction. Fig. S14c (ESI†) is from this control experiment and shows, as expected, clean SWCNT-DBCO comparable to those of Fig. S14a (ESI†). This confirms the successful synthesis of AuNP-decorated SWCNT through the new I-SPAAC reaction between SWCNT-DBCO and N_3-EG_4-AuNP.

Finally, sonication was employed to test the stability and resilience of the final hybrid material. A fraction of SWCNT–AuNP were dispersed in PBS pH 7.0 and ultra-sonicated for one hour. The TEM images obtained from these samples were compared with those of the freshly prepared SWCNT–AuNP and they did not show any appreciable difference either in the density of chemisorbed AuNP or in the AuNP size distribution. This supports the efficiency of our synthetic approach and the resilience of the resulting AuNP–CNT hybrid. The reaction of the N_3-EG_4-AuNP with DBCO as a model leads to efficient and total loading (complete reaction) on the AuNP. Because of this and the high effective concentration of the N_3 moiety on each AuNP we believe that every accessible DBCO on the DBCO-SWCNT reacts with N_3-EG_4-AuNP.

In summary, we introduce a simple and efficient copper-free interfacial strain-promoted alkyne–azide cycloaddition (I-SPAAC) reaction at the interface between different nanosystems: a new DBCO modified CNT and versatile *water-soluble* azide modified AuNP. This I-SPAAC reaction was fast and effective, leading to CNT homogeneously covered with small AuNP and to a robust and stable hybrid material thanks to the covalent bond that links the two nano-partners. Importantly, due to the nature of the AuNP ligands these hybrid materials are easily dispersed in aqueous environment to aid in use for a variety of applications as varied as gas sensors, catalysts, and as structural components of electrochemical sensors. The coupling-based strategy introduced here can be exploited for exploring and creating a wide variety of bioorthogonal nanostructured materials for device applications. For example, it is possible to take advantage of the intrinsic presence of carboxylic acid groups on the surface of carbonaceous material (*i.e.* graphene, nanodiamonds, glassy carbon) to introduce strained alkynes through the coupling reaction here described. These bioorthogonal materials would then be able to bind the azide-functionalized AuNP or other azide modified biomolecules through the I-SPAAC reaction.

We acknowledge NSERC Canada and UWO for financial support.

Notes and references

1 M. D. Best, *Biochemistry*, 2009, **48**, 6571.
2 J. C. Jewett and C. R. Bertozzi, *Chem. Soc. Rev.*, 2010, **39**, 1272.
3 M. F. Debets, S. S. Van Berkel, J. Dommerholt, A. J. Dirks, F. P. J. T. Rutjes and F. L. Van Delft, *Acc. Chem. Res.*, 2011, **44**, 805.
4 N. J. Agard, J. A. Prescher and C. R. Bertozzi, *J. Am. Chem. Soc.*, 2004, **126**, 15046.
5 E. Lallana, E. Fernandez-Megia and R. Riguera, *J. Am. Chem. Soc.*, 2009, **131**, 5748.
6 J. M. Baskin, J. A. Prescher, S. T. Laughlin, N. J. Agard, P. V. Chang, I. A. Miller, A. Lo, J. A. Codelli and C. R. Bertozzi, *Proc. Natl. Acad. Sci. U. S. A.*, 2007, **104**, 16793.
7 A. Kuzmin, A. Poloukhtine, M. A. Wolfert and V. V. Popik, *Bioconjugate Chem.*, 2010, **21**, 2076.
8 D. H. Ess, G. O. Jones and K. N. Houk, *Org. Lett.*, 2008, **10**, 1633.
9 J. C. Jewett, E. M. Sletten and C. R. Bertozzi, *J. Am. Chem. Soc.*, 2010, **132**, 3688.
10 J. Dommerholt, S. Schmidt, R. Temming, L. J. A. Hendriks, F. P. J. T. Rutjes, J. C. M. Van Hest, D. J. Lefeber, P. Friedl and F. L. Van Delft, *Angew. Chem., Int. Ed.*, 2010, **49**, 9422.
11 K. E. Beatty, J. D. Fisk, B. P. Smart, Y. Y. Lu, J. Szychowski, M. J. Hangauer, J. M. Baskin, C. R. Bertozzi and D. A. Tirrell, *ChemBioChem*, 2010, **11**, 2092.
12 N. E. Mbua, J. Guo, M. A. Wolfert, R. Steet and G.-J. Boons, *ChemBioChem*, 2011, **12**, 1911.
13 H. Koo, S. Lee, J. H. Na, S. H. Kim, S. K. Hahn, K. Choi, I. C. Kwon, S. Y. Jeong and K. Kim, *Angew. Chem., Int. Ed.*, 2012, **51**, 11836.
14 J. A. Johnson, J. M. Baskin, C. R. Bertozzi, J. T. Koberstein and N. J. Turro, *Chem. Commun.*, 2008, 3064.
15 A. Bernardin, A. Cazet, L. Guyon, P. Delannoy, F. Vinet, D. Bonnaffé and I. Texier, *Bioconjugate Chem.*, 2010, **21**, 583.
16 S. V. Orski, A. A. Poloukhtine, S. Arumugam, L. Mao, V. V. Popik and J. Locklin, *J. Am. Chem. Soc.*, 2010, **132**, 11024.
17 N. Chauhan, A. Singh, J. Narang, S. Dahiya and S. C. Pundir, *Analyst*, 2012, **137**, 5113.
18 J. Huang, X. Xing, X. Zhang, X. He, Q. Lin, W. Lian and H. Zhu, *Food Res. Int.*, 2011, **44**, 276.
19 D. Cai, Y. Yu, Y. Lan, F. J. Dufort, G. Xiong, T. Paudel, Z. Ren, D. J. Wagner and T. C. Chiles, *BioFactors*, 2007, **30**, 271.
20 Y. Guo, S. Guo, Y. Fang and S. Dong, *Electrochim. Acta*, 2010, **55**, 3927.
21 P. Gobbo and M. S. Workentin, *Langmuir*, 2012, **28**, 12357.
22 H. Liu, B. S. Mun, G. Thornton, S. R. Isaacs, Y.-S. Shon, D. F. Ogletree and M. Salmeron, *Phys. Rev. B*, 2005, **72**, 155430.
23 C. R. Henry, *Surf. Sci. Rep.*, 1998, **31**, 231.
24 A. Devadoss and C. E. D. Chidsey, *J. Am. Chem. Soc.*, 2007, **129**, 5370.

